

Plastinated nasal model: a new concept of anatomically realistic cast

Marc DURAND^{1,2,3,4}, *Jérémy POURCHEZ*^{3,5*}, *Bruno LOUIS*⁶, *Jean-François POUGET*⁷,
*Daniel ISABEY*⁶, *André COSTE*⁶, *Jean-Michel PRADES*^{2,3,4,8}, *Philippe RUSCH*^{2,3,4,8}, *Michèle COTTIER*^{2,3,4,8}

¹ Centre Hospitalier Emile Roux, ENT center, Le Puy en Velay, France

² Université Jean Monnet, Faculté de Médecine, IFR Inserm 143, F-42023, Saint-Etienne, France

³ LINA, F-42023, Saint-Etienne, France

⁴ Université de Lyon, F-42023, Saint-Etienne, France

⁵ Ecole Nationale Supérieure des Mines de Saint-Étienne, Centre Ingénierie et Santé, IFR Inserm 143, Saint-Etienne, France

⁶ INSERM U955, Institut Mondor de Recherche Biomédicale, Biomécanique Cellulaire et Respiratoire, PRES Paris-Est, Université Paris 12, Faculté de Médecine, Créteil, France

⁷ Clinique Mutualiste, Saint-Etienne, France

⁸ CHU de Saint-Etienne, F-42055, Saint-Etienne, France,

* Corresponding author: Tel: (+33) 4 77 42 01 80; Fax: (+33) 4 77 49 96 94;
E-mail address: pourchez@emse.fr

1 **SUMMARY.**

2 **Background:** For many years, several researchers have been interested in investigating
3 airflow and aerosol deposition in the nasal cavities. Nasal airways appear to be a complex
4 geometrical system. Thus, *in vitro* experimental studies are frequently conducted with more or
5 less biomimetic nasal replica.

6 **Aim:** This study is devoted to the development of anatomically realistic nose model with
7 bilateral nasal cavities, *i.e.* nasal anatomy, airway geometry and aerodynamic properties as
8 close as possible to *in vivo* behaviour.

9 **Methods:** A specific plastination technique of cephalic extremities was developed by the
10 Anatomy Laboratory at the Saint-Etienne University since the last 10 years. The plastinated
11 models obtained were anatomically, geometrically and aerodynamically validated using
12 several techniques (endoscopy, CT scans, acoustic rhinometry and rhinomanometry).

13 **Main results:** Our plastination model exhibited a high level of anatomic quality, *e.g.* a very
14 good mucosa preservation. Aerodynamical and geometrical investigations highlighted a
15 global behaviour of plastinated models perfectly in accordance with a nasal decongested
16 healthy subject.

17 **Conclusions:** The present plastination model provides a realistic cast of nasal airways, and
18 may be a useful tool for nasal flow, drug delivery and aerosol deposition studies.

19

20 **Keywords:** anatomic model, nasal airway cast, plastination, maxillary sinuses.

21 **Introduction**

22 Nowadays, nebulization is the preferred route for drug delivery in asthma and chronic
23 obstructive pulmonary disease. As therapeutic agents can be delivered directly to the
24 respiratory tract, the inhaled route offers smaller doses to be used and a more rapid onset of
25 action compared to systemic therapy. In this context, the practice of nasal drug delivery by
26 nebulization is also widely used in otorhinolaryngology, even if there is a lack of reliable data
27 concerning the evaluation of its efficacy [1]. To more accurately define the relevance of nasal
28 drug delivery, a better understanding of the deposition of nebulized drugs in the human nasal
29 cavity is required. Aerosol deposition may be evaluated using different nasal replica.

30 In broad outline, three main families of human nasal casts can be distinguished: “pipe
31 models” [2-4], plastic replicas [5-6] and models obtained from cadavers [7]. Unfortunately,
32 these usual experimental casts show specific restrictions: “pipe models” may not adequately
33 mimic the anatomy of the human cavity, plastic replicas can suffer from a lack of thin
34 anatomical details (such as the sinus ostium morphology), and models from cadavers induce
35 issues of time stability and biosecurity.

36 Thus, we propose to create a new concept of functional human plastinated nasal cast.
37 Plastination permits the preservation of anatomical specimens in a physical state approaching
38 that of the living condition. This technique was introduced by Dr. Gunther von Hagens in the
39 end of 1970s [8]. This process consists in replacing water and lipids in biological tissue by
40 curable polymers. Then, polymers are hardened resulting in dry, odorless and durable
41 anatomic specimen. Nevertheless, plastination is usually restricted to descriptive and
42 topographic studies of anatomy. That is why, the development of a specific plastination
43 protocol is needed in order to create for the first time a plastinated human model devoted to
44 functional studies (e.g. airflow and aerosol deposition experiments). To assess the relevance
45 of our new concept of plastinated nasal models, some preliminary *in vitro* studies were
46 performed. A first study highlights scintigraphic images of plastinated casts using a

47 technetium (^{99m}Tc)-labelled solution to investigate the penetration of aerosols inside
48 maxillary sinuses [9]. A second one allows to validate the ability of a Computational Fluid
49 Dynamic (CFD) software describing pressure drop and flow [10].
50 The technical specifications of the plastinated nasal model to develop are: anatomical features
51 as close as possible to *in vivo* human airways, time-stability to perform experimental
52 campaign during several years, water-washable to clean the specimen between tests,
53 accessibility of the maxillary sinuses to assess the aerosol deposition, easy handling daily, dry
54 odourless, biologically safe and transportable without restricted constraints. This study
55 presents an original plastination protocol as well as clinical, geometric and aerodynamic
56 characterisation of plastinated nasal airways models using several techniques (endoscopy, CT
57 scans, acoustic rhinometry and rhinomanometry).

58 **Materials and methods**

59 *Nasal specimens*

60 Three nasal specimens were successively plastinated. We used adult heads, one female
61 (specimen 1) and two males (specimens 2 and 3). On specimens 2 and 3, we carefully cut
62 away the lateral wall of the maxillary sinuses leading to access inside. Different steps
63 successively occurred (Table 1) during the plastination process: anatomical sampling, section,
64 fixation, dissection, dehydration and degreasing, polymer forced impregnation in a vacuum,
65 and then curing and polymerization.

66

67 *Fixation and anatomical dissection*

68 The first step of plastination consisted in anatomical sampling from a cadaver donated to the
69 Anatomy Laboratory of Saint-Etienne University. The cadavers were obtained from deceased
70 men or women whose last will and testament documented his wish to leave his body to the
71 Anatomy Laboratory. The cadavers were clinically checked by a qualified ENT specialist
72 prior to begin the anatomical sampling. After freezing the specimen at -80°C , a lateral-
73 paramedian section of the cephalic extremity may be carried out. This section allows to access
74 of the maxillary sinuses which nevertheless keep a normal volume and aerodynamic
75 behaviour. Besides, working only with this section offers also a significant time gain during
76 the plastination procedure because of a fast penetration of solvents into the anatomical
77 specimen. During the fixation step, the specimen was embalmed by immersion in a 10 % vol.
78 formaldehyde solution so as to halt decomposition. Long fixation duration, around 3 months,
79 was generally necessary to avoid tissue retraction phenomena during the polymer forced
80 impregnation stage. The temperature was maintained at 5°C during this fixation process.

81

82

83

84 *Dehydration and delipidation*

85 Removal of fat and water from tissues of fixed specimen was the stage in which the
86 specimens were immersed, under freezing conditions at -25°C , in several successive baths of
87 pure acetone. The acetone was used as a degreasing and dehydration agent because this
88 solvent was able to draw out all fats and water and replace them inside the cells. The
89 specimens were passed through several baths of acetone until water and lipids content of the
90 last acetone solution was less than 1%. Therefore, at least 4 baths of pure acetone were
91 required to fully delipidate a cephalic extremity beforehand sectioned. Duration of each
92 acetone bath varied between one and four weeks depending to the volume and tissue content
93 of the specimen to be plastinated as well as the bath number. Between one and two months
94 were generally necessary to satisfactorily dehydrate and degrease a specimen.

96 *Silicon forced impregnation*

97 Polymer forced impregnation under vacuum conditions was the key principle of plastination.
98 The temperature was always maintained at -25°C . We immersed the specimen in a silicon
99 solution bath (S10 Biodur[®]) placed in a vacuum chamber. We gradually reduced the pressure
100 until acetone boils. At this moment, acetone is vaporized and suctioned out of the tissue, and
101 continuously extracted from the specimen. The resulting negative pressure causes the silicon
102 solution to gradually permeate the tissue. A precise control of the depression applied versus
103 time was therefore absolutely essential and necessitated specific know-how. The duration of
104 the polymer forced impregnation was between 10 and 20 days.

106 *Silicon Curing*

107 After this impregnation, a gas curing takes place to polymerize silicon and thus to keep the
108 polymer inside the specimen tissue. The gas curing was carried out at room temperature in a
109 closed chamber. The hardening product (S6 Biodur[®]) was a liquid containing silicate with a

110 high saturated vapor pressure. It evaporates and builds up a gaseous atmosphere inside the
111 chamber. This active vapor reacts with the silicon at the specimen surface, and then the
112 polymer begins side to side-linkage. Rapidly, the outer surface of the specimen was cured
113 because of silicon polymerization. Over a period of time, the curing gas diffuses into the
114 specimen and polymerization proceeds deeper. After a one month period in contact with the
115 curing gas in a close environment, a final curing step begins. This final curing aimed at totally
116 hardening the center of the specimen.

117

118 *Anatomical and aerodynamic characterisation of plastinated nasal models*

119 The overall objective of the anatomic and aerodynamic characterisation consisted in:

120 ☛ Checking by nasofiberscopy the preservation of nasal airway anatomy during the
121 plastination protocol.

122 ☛ Performing CT-scans observations of the final plastinated models to evaluate and improve
123 the quality of the plastination procedure.

124 ☛ Evaluating the reliability of nasal cavity geometry (determined by acoustic rhinometry) and
125 airflow resistance (measured by rhinomanometry) of the final plastinated models compared to
126 *in vivo* data known from the literature.

127 The clinical anatomy study by nasofiberoscopic examinations (flexible Machida fiberscope,
128 Japan) were performed in the three specimens during all the plastination process: from the
129 anatomical sampling stage on the cadavers to the final curing step. This monitoring allows to
130 early detect any problem on the specimen during the 6 months duration of the plastination
131 procedure. Plastinated nasal models were also characterized using tomodensitometry (General
132 Electric Prospeed Advantage Scanner with Sun Sparc Solaris console) in the three specimens.
133 These techniques were performed on plastinated models in order to evaluate the preservation
134 of mucosa in the cast as well as to precisely define the geometrical characteristics of ostia and
135 maxillary sinus cavities.

136 The geometry of nasal cavities was also characterized using acoustic rhinometry in specimens
137 2 and 3 [10,11]. Briefly, the device consisted of two microphones (piezoresistive pressure
138 transducers 8510-B; Endevco France, Le Pré Saint-Gervais, France) and a horn driver
139 mounted on a wave tube (inner diameter: 1.2 cm and overall length: 22 cm) connected at one
140 end to a nostril of the model with a nosepiece, allowing tight closure of the nasal entrance.
141 The horn driver generated an acoustic wave, and the two microphones recorded the resulting
142 pressure. These digitized data were analyzed to obtain the cross-sectional areas of the nasal
143 airway as a function of the distance along the longitudinal axis, with a spatial step increment
144 of $\Delta L \approx 0.41$ cm. Each nasal fossa of plastinated specimens was separately examined leading
145 to the longitudinal area profiles from the tip of the nostril to the middle meatus region.
146 Finally, rhinomanometry was used to provide an objective quantification of nasal airway
147 resistance in specimens 2 and 3. Steady flow was measured with a Fleisch pneumotachograph
148 (Lausanne, Switzerland) coupled to a differential pressure transducer (Validyne DP45,
149 Northridge, CA) by short tubes allowing to estimate the pressure drop. Inspiratory flows for
150 the three different gases were generated by a negative pressure generator made of a turbine
151 rotating at a constant adjustable speed which was connected to the nasopharyngeal extremity
152 of the plastinated airway model. Each nasal cavity was investigated individually. The pressure
153 difference and transnasal airflow were simultaneously measured. The aerodynamic resistance
154 was defined as the ratio of pressure drop across the nose over the volume rate of nasal airflow,
155 when the transnasal pressure reached 1 cmH₂O. To measure the airflow resistance of the right
156 nasal cavity, maxillary sinus cavity were in “closed” position and the left nostril was
157 occluded.

158 **Results**

159 *Overall observations*

160 In this paper we focused on 3 specimens allowing to exhibit the improvement of the
161 plastination protocol with time (Fig. 1). Moreover, we obviously examined an improvement
162 of subcutaneous and mucosa preservation between specimens 1 and 3. As a matter of fact, the
163 specimen 1 perfectly showed a high tissue retraction because of bad polymer forced
164 impregnation during first tests. On the contrary, the specimen 3 highlighted a very low tissue
165 retraction and an astonishing preservation, certainly the closest possible to living tissue. Thus,
166 these observations appeared as a sign of a significant improvement of the plastination
167 procedure with time.

169 *Nasofiberoscopy*

170 The clinical anatomy study showed that the plastinated nasal specimens 2 and 3 were very
171 similar to living anatomical conditions daily observed by ENT physicians. As a matter of fact,
172 the coloration was clearly checked and all anatomical details were well-preserved. As an
173 example, we clearly put in evidence in the specimen 2 a *concha bullosa* referring to the
174 pneumatization of the middle turbinates of the right nasal cavity (Fig 2). Endoscopic
175 observations also lead to confirm that the final plastination protocol, corresponding to the
176 elaboration of specimen 3, guarantees an excellent preservation of nasal airways anatomy.

178 *Tomodensitometry*

179 CT scans confirmed the high preservation of nasal airway anatomy of specimen 3. On the one
180 hand, 3D reconstruction and virtual endoscopy from imaging data exhibited high quality of
181 anatomy closed to living conditions (Fig 3). On the other hand, we emphasized a significant
182 increase of the mucosa thickness on the turbinates of the specimen 3 (Fig 3 and 4). Thus, the
183 mucosa preservation of the turbinates was higher in the case of specimen 3 thanks to the

184 plastination procedure improvement. Finally, specimen 3 also exhibited very dissimilar
185 maxillary sinus ostium morphologies (Fig 4). Indeed, while the right maxillary sinus ostium
186 appeared as anatomically usual, the left maxillary sinus ostium was doubtless abnormally
187 short and broad. In particular, the diameter of the left maxillary sinus ostium was three times
188 higher compared to the right maxillary sinus ostium.

189

190 *Acoustic rhinometry*

191 The acoustic rhinometry was found to reasonably resolve the airways geometry of the
192 plastinated casts. Concerning the specimen 2, characterized by pneumatised middle turbinate
193 (*i.e.* a concha bullosa) in the right nasal cavity, the comparison of areas obtained by acoustic
194 reflexion and by 3D reconstruction and then image analysis were previously described in [12].
195 Both methods provided a relatively good agreement mainly in the anterior part of the nose
196 because of the acoustic method lead to overestimate the area lying beyond the ostium. The
197 specimen 3 was also investigated thanks to this technique (Fig 5). Whatever the plastinated
198 specimen examined, we always found a minimal cross-sectional area around 0.5 cm^2 and a
199 cross-sectional area higher than 1.5 cm^2 from the middle meatus region.

200

201 *Rhinomanometry*

202 First of all, we measured the resistance of each nasal cavity separately while the opposite
203 nostril was occluded. From the pressure vs flow curves, the unilateral airflow resistances
204 found on specimen 3, for left and right nasal cavities, were perfectly similar at $0.18 \text{ Pa.s.cm}^{-3}$
205 (*i.e.* $1.8 \text{ cmH}_2\text{O.s.L}^{-1}$). The bilateral airflow resistance was logically measured at a lower
206 value compared to unilateral resistances, around $0.13 \text{ Pa.s.cm}^{-3}$. A similar investigation of
207 airflow resistance was also performed on specimen 2 (Table 2). We found a rise of airflow
208 resistance for the right nostril (0.21 versus $0.16 \text{ Pa.s.cm}^{-3}$ for the left nasal cavity).

209 **Discussion**

210 *Plastinated nasal casts versus living noses*

211 To validate this new concept of anatomical realistic cast, the reliability of plastinated nasal
212 model should be harshly examined by comparison with usual living anatomy as well as *in*
213 *vivo* geometric and aerodynamic data of healthy subject. A plastinated model devoted to
214 functional studies needs a specific plastination protocol. In fact, a main challenge consists in a
215 plastination technique enables to ensure a very low degree of tissue retraction. Therefore, high
216 nasal mucosa preservation remains a key point in order to provide conserved specimen with
217 an appearance remaining close to live anatomy. Endoscopic and CT scans observations lead
218 to show a significant improvement of the plastination procedure between the specimen 1 and
219 3. We also proved that our final plastination protocol, *i.e.* the elaboration of specimen 3, leads
220 to an excellent conservation of nasal airways anatomy with a high mucosa preservation. We
221 support the conclusion that the improvement of our plastination protocol with time allows to
222 obtain plastinated specimen not too far from live anatomy.

223 Acoustic rhinometry is frequently used to determine *in vivo* the nasal cross-sectional areas
224 through acoustic reflexion [11]. It is a reliable and non invasive mean in order to assess the
225 first six centimetres of the nasal fossa anatomy [13]. Although this method has been used in
226 clinical practice, some authors underline its potential limitations in the case of sudden large
227 area changes in the space [14], or about the cross-sectional areas posterior to a significant
228 constriction [12]. The acoustic rhinometry, performed on specimen 3, emphasized a perfect
229 symmetry of right and left nasal cavities from the nostril to the ostium of maxillary sinus (Fig
230 5). Moreover, if we compare the acoustic rhinometry results on plastinated models with data
231 performed *in vivo*, the closest correlations have been noted between the plastinated nasal casts
232 and the geometrical information obtained in healthy subjects after the application of a nasal
233 decongestant. In particular, a good correlation was observed between the cross-sectional areas

234 generated with the plastinated specimens 2 and 3 (Fig. 5) and postdecongested acoustic
235 rhinometry data in healthy subjects described in [15].

236 Rhinomanometry is a well-established and reliable technique that measures nasal patency in
237 terms of nasal airflow and resistance to airflow [16,17]. The unilateral airflow resistances
238 measured on specimen 3, for left and right nasal cavities, were similar. This tendency was
239 consistent with the geometry of nasal cavity investigated by acoustic rhinometry showing
240 identical longitudinal area profile for both left and right nasal cavities (Fig 5). We also
241 emphasized a significant rise of airflow resistance for the right nostril of specimen 2. This
242 asymmetry can easily be explained by the presence of a *concha bullosa* in the right nasal
243 cavity of specimen 2. Besides, the measured pressure–flow relationship reflects the functional
244 status of the nasal airway. Thus, this technique was usually carried out to measure the nasal
245 resistance before and after surgery for nasal resistance. From the literature a consensus seems
246 to be reached since an unilateral resistance greater than $0.35 \text{ Pa}\cdot\text{s}\cdot\text{cm}^{-3}$ suggests clinically
247 significant nasal obstruction. As a general rule, the nasal resistance can be categorized into
248 four grades [18]. From the clinical standpoint, the nasal resistance below $0.19 \text{ Pa}\cdot\text{s}\cdot\text{cm}^{-3}$
249 corresponding to grade 1, indicates a subject free from nasal obstruction. Besides, above 4
250 $\text{Pa}\cdot\text{s}\cdot\text{cm}^{-3}$ corresponding to grade 4 the airflow resistance indicates a subject suffering from
251 the very severe or complete nasal obstruction. Regarding to this nasal resistance scale, as the
252 unilateral airflow resistances obtained in the specimen 3 was around $0.18 \text{ Pa}\cdot\text{s}\cdot\text{cm}^{-3}$, the
253 plastinated replica presents an airflow resistance similar to that of a decongested healthy
254 subject.

255 *Plastinated nasal casts versus other nasal replicas*

256 According to the specific advantages and drawbacks of experimental nasal models found in
257 the literature, we must examine if a human plastinated nasal model leads to a significant
258 scientific breakthrough. To simulate nasal airways, experimental casts with increasing
259 complexity can be used. The “pipe model” [2-4] is usually a two compartment model where

260 pipes represent nasal and sinus cavities. Following this overall strategy, Moller *et al.*
261 elaborated a polyoxymethylene replica where sinuses were modelled by cylindrical glass vials
262 [2]. Cakmak *et al.* developed a model consisting of a brass pipe with a short neck that
263 branched off and opened into an enclosed cavity [3]. Maniscalco *et al.* built a model
264 composed of a syringe (representing the sinus) connected horizontally to a plastic cylinder
265 (representing the nasal cavity) [4]. Although “pipe models” [2-4] are very useful to collect
266 data in a first approach, it remains unclear how relevant the data are to study *in vivo* drug
267 delivery. Obviously, “pipe models” may not adequately mimic the complex anatomy of the
268 human nasal cavities *in vivo*. Especially, these casts may underestimate the difficulty of
269 getting nasally administrated drug beyond the nasal valve and front surfaces of the turbinate
270 because of a lack of anatomical features. As a result, the plastinated nasal cast seems to be
271 very useful to study aerosol depositions and is without doubt preferable to any “pipe model”.

272 To improve biomimetic geometry of the experimental replicas, plastic/silicon models [5,6]
273 can also be reconstructed from medical imaging data. As example, Schreck *et al.* used
274 magnetic resonance images (4 mm apart) to make a threefold-enlarged plastic cast of a left
275 nasal cavity [5]. Computed tomography scans coupled with rapid prototyping technique allow
276 to elaborate models such as the silicon right nasal cavity developed by Kelly *et al.* [6].
277 Moreover, the plastic/silicon models [5,6] reconstructed from imaging data significantly
278 improve the biomimetic geometry of replicas. Some replica was created from a living person
279 (*i.e.* from CT scans of the nasal cavities of an adult volunteer) and presents both nasal cavities
280 for numerical simulations [19]. Nevertheless these plastic/silicon models point out specific
281 restrictions. Besides, the spatial resolution of imaging techniques (around some millimeters)
282 as well as the smoothing procedure imposed by the reconstruction process, could considerably
283 compromise the reliability of the very local anatomical details. Indeed, a three-dimensional
284 reconstruction made from CT scans images too spaced may prevent the capturing of thin
285 anatomical features, such as the maxillary sinus ostium whose internal diameter does not

286 exceed 2-5 mm. Thus, this lack of very thin anatomical details observed in plastic models can
287 strongly affect the replica behaviour especially in term of sinus ventilation or aerosol
288 deposition in sinus cavities.

289 Finally, it certainly makes more sense to compare plastinated nasal casts with other models
290 which are obtained from cadavers. As a matter of fact, these latter emphasize a high level of
291 anatomical features. Nevertheless, they also induce specific issues of time stability (*i.e.* a
292 relative short-term use to avoid tissue degradation) and biosecurity (*i.e.* with reference to
293 handling, transportation, formaldehyde vapours ...) [7]. All things considered, to carry out
294 dozens of experimental tests on a relatively long period (*e.g.* many months or years to develop
295 new prototypes of nebulizers and to assess their aerosol deposition in specific nasal regions of
296 a same human nose), the plastinated nasal cast is a very helpful tool. In other words the
297 plastinated cast appears as an interesting compromise between on the one hand the anatomical
298 quality of models from cadavers, and on the other hand biosecurity, stability and easy-to-use
299 of plastic nasal replicas.

300 But the plastinated nasal replica exhibits some constraints. It is obvious that the vasoactive
301 role of the mucosa present in living tissue can never be reproduced by plastination technique.
302 Besides, by contrast with plastic replica, nothing can be temporarily removed from such a
303 plastinated cast (*e.g.* the inferior turbinate or the uncinat process) to study the effects on flow
304 and cross-sectional. Only addition can be made, for instance to enhance the thickness of the
305 mucosa. However, to assess the impact of some anatomical parameters, “pathologic” nasal
306 specimens (with cartilaginous deviation, functional surgery designed to enlarge the nasal
307 fossa) can be plastinated and thus results are compared to data obtained on “normal”
308 plastinated nasal casts. We must underline that the main drawbacks of plastinated replicas are
309 the high-duration to elaborate one cast (around six months) as well as the specific plastination
310 know-how needing many years of operational experience. Considering this limitation, even if
311 approximately 150 laboratories in the world frequently use the plastination technique, the

312 plastinated nasal cast is not a tool which can be applied easily and quickly without previous
313 experiences on plastination procedures. Nevertheless, the authors build relationships with a
314 wide range of stakeholders and research groups to encourage and promote know-how transfer
315 and experience sharing. We hope that this knowledge dissemination activities dealing with
316 this specific plastination technique will allow the plastinated nasal casts to become more and
317 more accessible. However, even if plastination appears as a tedious and complex technique,
318 we support the conclusion that plastinated human nose casts allow to a significant scientific
319 breakthrough compared to existing experimental nasal replicas.

320 **Conclusion**

321 A novel anatomically realistic nasal cast with bilateral nasal cavities, based on plastination
322 technique, was found suitable. We demonstrate that the nasal plastinated model allow to avoid
323 tissue retraction as well as to well preserve anatomical details. The comparison of the
324 geometric and aerodynamic characteristics of the specimen 3 with *in vivo* data clearly
325 indicates that the plastinated cast acceptably match a decongestant healthy subject. All things
326 considered, we succeed to develop a cast with similar advantages of models from cadavers
327 (*e.g.* high anatomical quality, biomimetic airways geometry and airflow resistance) but
328 without theirs specific drawbacks (*e.g.* low time-stability, biosecurity issues).

329 By way of conclusion, the development of anatomically realistic plastinated nose models with
330 bilateral nasal cavities is certainly a valuable tool to bring a sound-knowledge of the accurate
331 role of anatomical parameters (ostium morphology, functional endoscopic sinus surgery) to
332 differential deposition of aerosols in the maxillary sinus by particle size, or to validate CFD
333 software which will be used to predict the functional effect of a treatment (*e.g.* functional
334 surgery designed to enlarge the nasal fossa ...).

335 **References**

- 336 1. Bonfils P. L'aérosolthérapie par nebulisation en oto rhino laryngologie. *Ann. Otolaryngol.*
337 *Chir Cervicofac* 1997 ; 114:147-156.
- 338
- 339 2. Möller W, Schuschnig U, Meyer G, Mentzel H, Keller M. Ventilation and drug delivery to
340 the paranasal sinuses: studies in a nasal cast using pulsating airflow. *Rhinology* 2008; 46:213-
341 220.
- 342
- 343 3. Cakmak O, Celik H, Cankurtaran M, Buyuklu F, Ozgirgin N, Ozluoglu LN. Effects of
344 paranasal sinus ostia and volume on acoustic rhinometry measurements: a model study. *J*
345 *Appl Physiol* 2003; 94:1527-1535.
- 346
- 347 4. Maniscalco M, Sofia M, Weitzberg E, Lundberg JO. Sounding airflow enhances aerosol
348 delivery into paranasal sinuses. *Eur J Clin Invest* 2006; 36:509-513.
- 349
- 350 5. Schreck S, Sullivan KJ, Ho CM, Chang HK. Correlation between flow resistance and
351 geometry in a model of the human nose. *J Appl Physiol* 1993; 75:1767-1775.
- 352
- 353 6. Kelly JT, Prasad AK, Wexler AS. Detailed flow patterns in the nasal cavity. *J. Appl.*
354 *Physiol.* 2000; 51:5-19.
- 355
- 356 7. Hilton C, Wiedmann T, St Martin M, Humphrey B, Schleiffarth R, Rimel F. Differential
357 deposition of aerosols in the maxillary sinus of human cadavers by particle size. *Am J Rhinol*
358 2008; 22:395-398.
- 359

- 360 8. von Hagens G. Impregnation of soft biological specimens with thermosetting resins and
361 elastomer. *Anat Rec* 1979; 194 :247-255.
- 362
- 363 9. Durand M, Rusch P, Granjon D, Chantrel G, Prades JM, Dubois F, Esteves D, Pouget JF,
364 Martin C. Preliminary study of the deposition of aerosol in the maxillary sinuses using a
365 plastinated model. *J Aerosol Med* 2001; 14:83-93.
- 366
- 367
- 368
- 369 10. Croce C, Fodil R, Durand M, Sbirlea-apiou G, Caillibotte G, Papon JF, Blondeau JR,
370 Coste A, Isabey D, Louis B. In vitro experiments and numerical simulations of airflow in
371 realistic nasal airway geometry. *Ann Biomed Eng* 2006; 34:997-1007.
- 372
- 373 11. Louis B, Glass G, Kresen B, Fredberg. Airway area by acoustic reflexion: the two-
374 microphone method. *J Biomech Eng* 1993; 115:278-285.
- 375
- 376 12. Cankurtaran M, Celik H, Cakmak O, Ozluoglu LN. Effects of the nasal valve on acoustic
377 rhinometry measurements: a model study. *J Appl Physiol* 2003; 94:2166-2172.
- 378
- 379 13. Cole P. Acoustic rhinometry and rhinomanometry. *Rhinology* 2000; 16: 29-34
- 380
- 381 14. Tomkinson A, Eccles R, acoustic rhinometry: an explanation of some common artefacts
382 associated with nasal decongestion. *Clin Otolaryngol Allied Sci* 1998; 23:20-26.
- 383

- 384 15. Corey JP, Gungor A, Nelson R, Fredberg J, Lai V, A comparison of the nasal cross-
385 sectional areas and volumes obtained with acoustic rhinometry and magnetic resonance
386 imaging, *Otolaryngol. Head Neck Surg* 1997; 117:349-354.
387
- 388 16. Cole P. Rhinomanometry 1988 – practice and trends. *Laryngoscope*, 1989; 99:311-315.
389
- 390 17. Coste A, Lofaso F, d'Ortho MP, Louis B, Dahan E, Peynegre R, Harf A. Protruding the
391 tongue improves posterior rhinomanometry in obstructive sleep apnoea syndrome. *Eur Respir*
392 *J* 1999; 14:1278-1282.
393
- 394 18. Soga T, Nakata S, Yasuma F, Noda A, Sugiura T, Yatsuya H, Koike Y, Ozaki N,
395 Nakashima T. Upper airways morphology in patients with obstructive sleep apnea syndrome:
396 effects of lateral positioning, *Auris Nasus Larynx*, 2009; 36:305-309.
397
- 398 19. Pless et al. Numerical simulation is a method displaying a real environment within a
399 computational model. *Am J Rhino* 2004; 18: 357

Table 1

Main stages of the plastination process	Keypoints of each stage	Global duration of each stage
Anatomical sampling	Post-mortem deadline within 24 hours	~ 3 hours
Lateral section of specimens	Freezing at -80°C	~ 3 days
Fixation and dissection	Embalming by immersion at 5°C in a 10 % formaldehyde solution	~ 3 months
Dehydration and degreasing	At least 4 successive baths of pure acetone at -25°C	~ 1-2 months
Polymer vacuum-forced impregnation	Immersion of the specimen in a silicon bath at -25°C, well-controlled depression applied	~ 10-20 days
Polymer hardening	Two step curing process and frequently manicured of the specimen when polymer oozing	~ 2-3 months

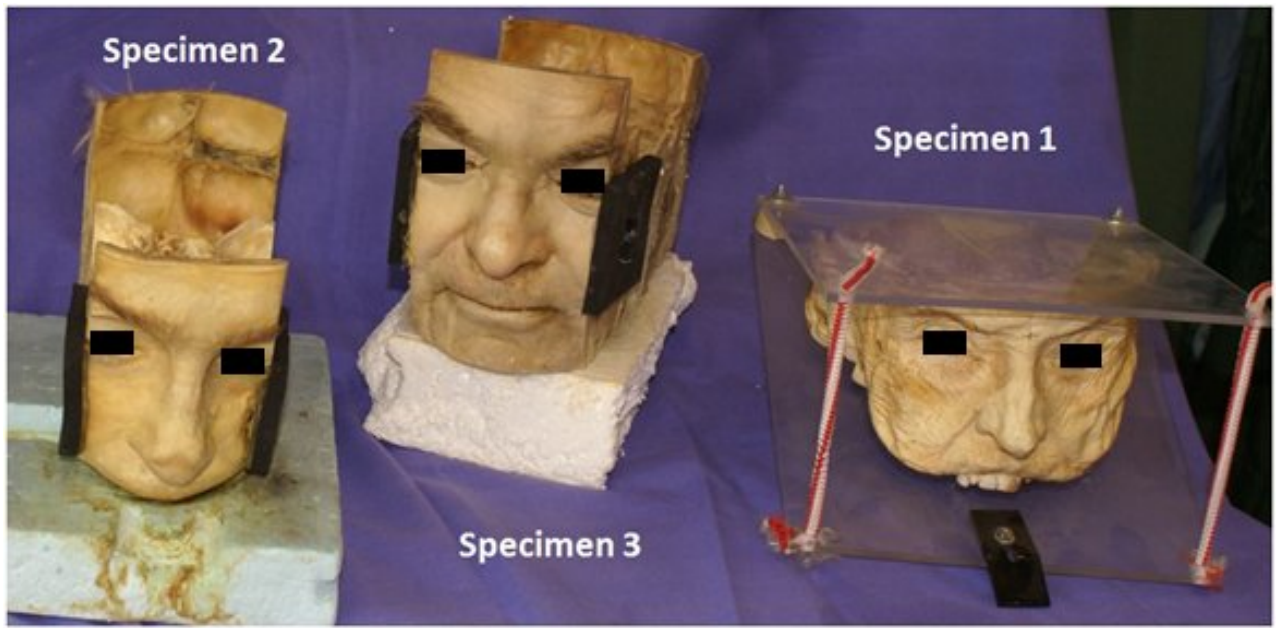
402

Table 1: Overall description of the plastination procedure developed.

403

404

Figure 1



405

406 Figure 1: Example of three plastinated nasal models elaborated thanks to our specific
407 plastination procedure.

408

409

Figure 2

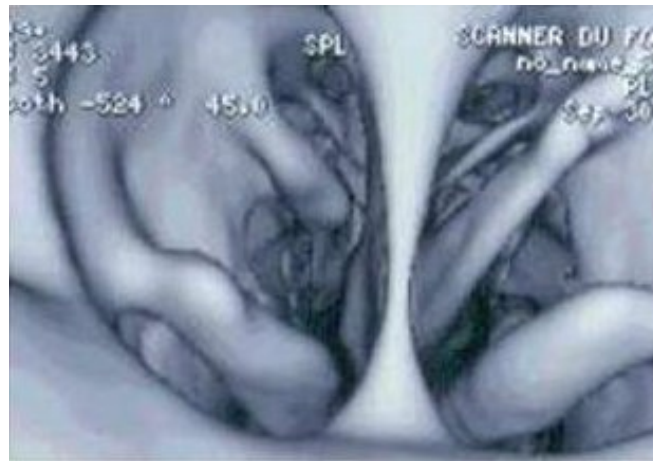


410

411 Figure 2: Nasofiberoscopy examination of the plastinated specimen 2. Observation of a
412 *concha bullosa* of the middle turbinates on the right nasal cavity

413

Figure 3

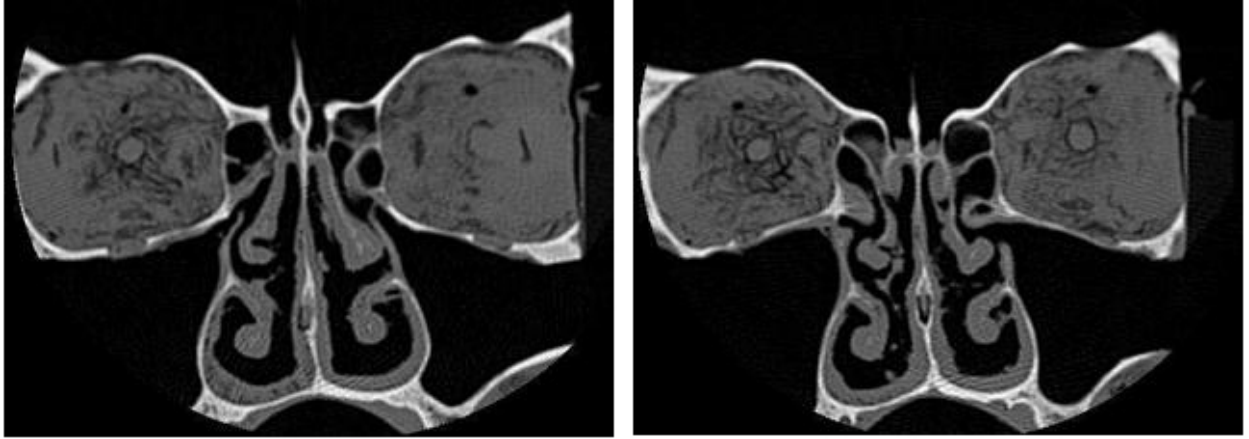


414

415 Figure 3: Virtual endoscopy from CT scans of the plastinated specimen 2: Posterior view of
416 choanae, visualization of nasal wall as well as the middle and inferior turbinates.

417

Figure 4



418

419 Figure 4: CT scans performed on the specimen 3. Observation of the high preservation of the
420 mucosa and of the different morphology of the maxillary ostia on both side.

Figure 5

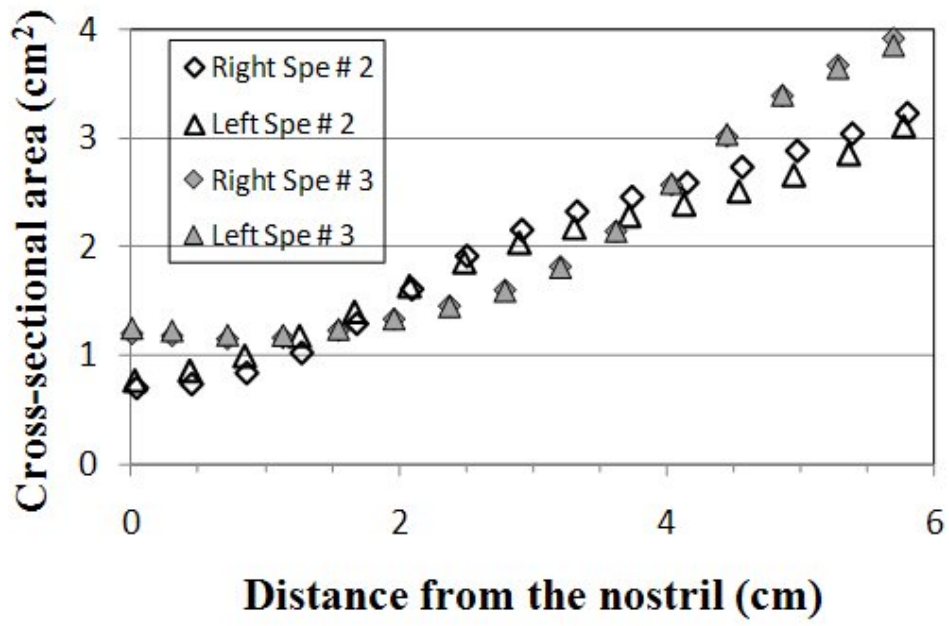


Figure 5: Comparison of acoustic rhinometry results obtained on specimens 2 and 3.

424

Table 2

	Specimen 2	Specimen 3
Bilateral	0.115 Pa.s.cm ⁻³	0.13 Pa.s.cm ⁻³
Right	0.21 Pa.s.cm ⁻³	0.18 Pa.s.cm ⁻³
left	0.16 Pa.s.cm ⁻³	0.18 Pa.s.cm ⁻³

425

426 Table 2: Comparison of airflow resistance investigated by rhinomanometry obtained on
427 specimens 2 and 3.

428
429